Study of the ^{14}Be Continuum: Identification and Structure of its Second 2^+ State

Yu. Aksyutina,[1] T. Aumann,[2,1] K. Boretzky,[1] M. J. G. Borge,[3] C. Caesar,[2,1] A. Chatillon,[1] L. V. Chulkov,[1,4] D. Cortina-Gil,[5] U. Datta Pramanik,[6] H. Emling,[1] H. O. U. Fynbo,[7] H. Geissel,[1] A. Heinz,[8] G. Ickert,[1] H. T. Johansson,[8] B. Jonson,[8] R. Kulessa,[9] C. Langer,[1] T. LeBleis,[1] K. Mahata,[1] G. Münzenberg,[1] T. Nilsson,[8] G. Nyman,[8] R. Palit,[10] S. Paschalis,[2] W. Prokopowicz,[1] R. Reifarth,[1,10] D. Rossi,[1,*] A. Richter,[2] K. Riisager,[7] G. Schrieder,[2] H. Simon,[1] K. Sümmerer,[1] O. Tengblad,[3] R. Thies,[8] H. Weick,[1] and M. V. Zhukov[8]

[1]*GSI Helmholtzzentrum für Schwerionenforschung GmbH, ExtreMe Matter Institute, EMMI, D-64291 Darmstadt, Germany*
[2]*Institut für Kernphysik, Technische Universität, D-64289 Darmstadt, Germany*
[3]*Instituto de Estructura de la Materia, CSIC, ES-28006 Madrid, Spain*
[4]*Kurchatov Institute, RU-123182 Moscow, Russia*
[5]*Universidade de Santiago de Compostela, ES-15782 Santiago de Compostela, Spain*
[6]*Saha Institute of Nuclear Physics, 1/AF Bidhannagar, Kolkata IN-700064, India*
[7]*Department of Physics and Astronomy, University of Aarhus, DK-8000 Aarhus, Denmark*
[8]*Fundamental Fysik, Chalmers Tekniska Högskola, SE-41296 Göteborg, Sweden*
[9]*Instytut Fisiki, Uniwersytet Jagelloński, PL-30-059 Krakóv, Poland*
[10]*Institut für Kernphysik, Johann-Wolfgang-Goethe-Universität, D-60486 Frankfurt, Germany*

(Received 1 October 2013; revised manuscript received 1 November 2013; published 9 December 2013)

The coupling between bound quantum states and those in the continuum is of high theoretical interest. Experimental studies of bound drip-line nuclei provide ideal testing grounds for such investigations since they, due to the feeble binding energy of their valence particles, are easy to excite into the continuum. In this Letter, continuum states in the heaviest particle-stable Be isotope, ^{14}Be, are studied by employing the method of inelastic proton scattering in inverse kinematics. New continuum states are found at excitation energies $E^* = 3.54(16)$ MeV and $E^* = 5.25(19)$ MeV. The structure of the earlier known 2^+_1 state at 1.54(13) MeV was confirmed with a predominantly $(0d_{5/2})^2$ configuration while there is very clear evidence that the 2^+_2 state has a predominant $(1s_{1/2}, 0d_{5/2})$ structure with a preferential three-body decay mechanism. The region at about 7 MeV excitation shows distinct features of sequential neutron decay via intermediate states in ^{13}Be. This demonstrates that the increasing availability of energetic beams of exotic nuclei opens up new vistas for experiments leading towards a new understanding of the interplay between bound and continuum states.

DOI: 10.1103/PhysRevLett.111.242501 PACS numbers: 25.40.Cm, 27.20.+n

Modern subatomic physics has in recent years experienced rapid technical developments resulting in clean, intense energetic beams of exotic nuclei [1]. As a consequence, this field of physics is literally bursting with new ideas to study nuclei at the limits of stability. Experiments with energetic radioactive beams, with half-lives down to the submillisecond region, reacting with various stable targets, allow studies of the structure of nuclei even at the extreme limits of stability. The technique, referred to as inverse kinematics has opened up the possibility to perform sophisticated reaction experiments with exotic nuclei. A subject of strong current theoretical interest is the coupling of bound states to continuum states in loosely bound nuclei. In this Letter, new data about quantum continuum states are presented. With a beam of ^{14}Be, inelastic proton scattering in inverse kinematics has been studied. We show new data identifying new resonances in the continuum with decay patterns starting with genuine three-body breakup at low energy to turn over to sequential decay via intermediate resonances at higher energy. ^{14}Be is the lightest member of the $N = 10$ isotones and the bare fact that it is possible to identify and assign the quantum signature of new continuum states demonstrates how modern experimental techniques push the frontier of nuclear physics.

A large matter radius for ^{14}Be [2,3], a narrow momentum distribution of ^{12}Be fragments after its fragmentation [4], electromagnetic dissociation (EMD) cross section [5], and a small Coulomb displacement energy between ^{14}Be(g.s) and its isobaric-analog state [6] are observations that characterize ^{14}Be as a nucleus with the presence of a spatially extended neutron halo with a large $(1s_{1/2})^2$ admixture.

With a two-neutron separation energy in ^{12}Be about a factor of 3 larger than in ^{14}Be and with ^{13}Be unbound, it is natural to model ^{14}Be as a ^{12}Be + n + n system. However, calculations within such a model, assuming a closed p shell in ^{12}Be, fail since they predict that the ground state of ^{13}Be should be bound [7,8]. Furthermore, a calculation [9], which had been successful for ^{11}Li, shows a mutual inconsistency between the experimentally determined binding energy, radius, and EMD energy spectrum.

A plausible explanation for this could be that ^{12}Be is not a good core. There are indeed convincing experimental results and theoretical predictions for ^{12}Be that favor a model where only small components of the ground-state wave function belong to the lowest shell-model configuration [10,11]. In such a description of ^{12}Be one assumes a ^{10}Be core with a closed $p_{3/2}$ subshell, and two valence neutrons in mixed s, p, and d configurations (see Ref. [12] and references therein). Such a model extended to ^{14}Be would allow us to consider it as a five-body system with four valence neutrons outside the ^{10}Be core.

The data presented here were obtained by inelastic proton scattering on ^{14}Be in inverse kinematics. A 304 MeV/u ^{14}Be beam was directed towards a liquid hydrogen target and the reaction products were detected in the ALADIN-LAND setup [13]. Coincidences between ^{12}Be and two neutrons provided momentum four vectors used in the analysis. The resolution of the momenta measured transverse to the beam direction was 2.7 MeV/c for neutrons and 35 MeV/c for fragments and in longitudinal direction 6.9 MeV/c for neutrons and 55 MeV/c for fragments, respectively. kinetic energy, that is, the relative energy, E_{fnn}, in the three-body $^{12}\mathrm{Be} + n + n$ system, as well as the fractional energies in the fragment-neutron ($\epsilon_{fn} = E_{fn}/E_{fnn}$) and the neutron-neutron ($\epsilon_{nn} = E_{nn}/E_{fnn}$) subsystems, were determined. The background was measured with an empty target container. The E_{fnn} experimental resolution, given as $0.18E_{fnn}^{0.75}$, and the overall detection efficiency were obtained from Monte Carlo simulations using measured LAND responses [14], and the simulations were used to make corrections for one-neutron events misidentified as two-neutron events.

The relative-energy spectrum, $d\sigma/dE_{fnn}$, is shown in Fig. 1. The strong increase of the cross section towards lower energies is due to the known 2_1^+ state at $E_r = 0.28(1)$ MeV [15]. The low-energy cutoff in the spectrum (see experimental points with error bars) is due to vanishing detection efficiency below $E_{nn} = 200$ keV, which limits the observation of the 2_1^+ state to its upper tail. The solid blue line is an interpretation of the $d\sigma/dE_{fnn}$ spectrum as consisting of three Breit-Wigner shaped resonances together with a contribution from unresolved resonances at higher energies (the dashed curve). The collected statistics made it, however, impossible to perform a least-square fit with all parameters left free. This problem was overcome by performing an iterative fitting procedure, which resulted in a $\chi^2/N = 27.9/35$. The curves in Fig. 1 show the detailed outcome of the analysis and the values of the final parameters for the resonances are given in Table I.

Even if only the tail of the 2_1^+ state is observed, an estimate of the cross section for the excitation of this resonance can be extracted. With a systematic uncertainty of about 20%, the derived cross section is $\sigma = 5.1(1.2)$ mb. This may be compared with the result of $\sigma = 12.5(1.6)$ mb obtained in the same reaction

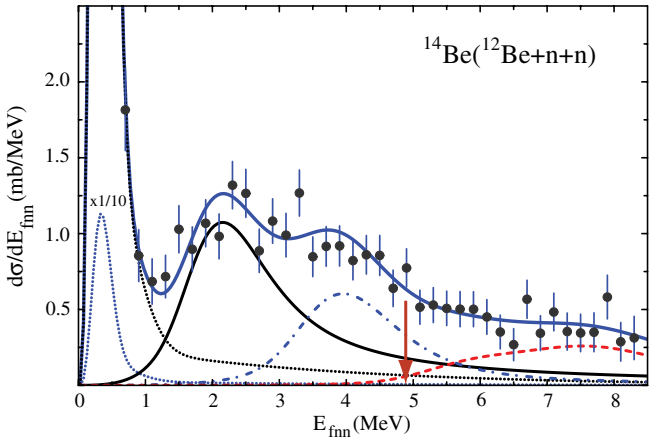

FIG. 1 (color online). Relative-energy spectrum ($d\sigma/dE_{fnn}$) of the $^{12}\mathrm{Be} + n + n$ system after inelastic scattering of 304 MeV/u ^{14}Be in a liquid hydrogen target. The curves show the decomposition of the spectrum into Breit-Wigner shaped resonances, with the experimental resolution taken into account. The arrow indicates the position of the four-neutron decay threshold.

at 69 MeV/nucleon [16]. As expected, it scales with the energy dependence of the nucleon-nucleon cross section.

The spin and parity assignments for the observed states were obtained from an analysis of the distributions of fractional energies, $W(\epsilon_{fn})$ and $W(\epsilon_{nn})$, derived from events in the regions $0.5 < E_{fnn} < 1$ MeV and $2 < E_{fnn} < 3$ MeV and displayed in Figs. 2(a)–2(d). A three-body decay may be described by two limiting cases of possible three-body decay modes. First, a sequential decay mode, where the three-body breakup proceeds via intermediate two-body resonances with lifetimes longer than that required for the particles to pass the interaction zone. The R-matrix formalism may effectively be used in this case. Second, few-body methods are needed to describe decays not passing through resonances in any binary subsystem. Such a genuine three-body decay mode is sometimes referred to as democratic decay [17]. The distributions displayed in Fig. 2 were analyzed under the assumption of democratic decay. It has been shown [18] that at low E_{fnn} only terms with the lowest possible angular momenta, consistent with selection rules, are needed

TABLE I. Resonance parameters for excited states in ^{14}Be. Statistical uncertainties are given.

I^π	E_r MeV	E^* MeV	Γ MeV	σ mb
2_1^+	0.28(1)[a,b]	1.54(13)[b]	0.025[a]	5.07(58)
2_2^+	2.28(9)	3.54(16)	1.5[a]	2.57(19)
(3^-)	3.99(14)	5.25(19)	1.0[a]	1.35(16)

[a]parameters were fixed.
[b]taken from Ref. [15].

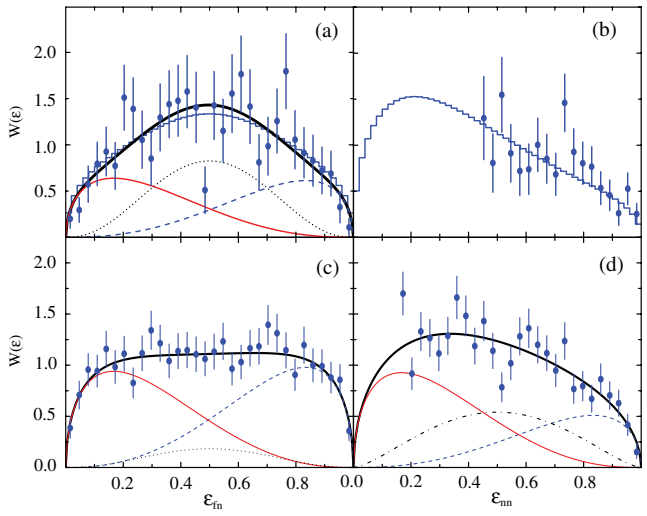

FIG. 2 (color online). The normalized distributions of fractional energies, $W(\epsilon_{fn})$ (a),(c) and $W(\epsilon_{nn})$ (b),(d), obtained in the energy regions $0.5 \leq E_{fnn} \leq 1$ MeV (a),(b) and $2 \leq E_{fnn} \leq 3$ MeV (c),(d). The thick solid line shows the fit by using Eq. (1), and the histograms display the result of a Monte Carlo simulation with the experimental resolution taken into account. The contributions from partial waves with different ℓ values are shown as lines: thin-solid–[0, 2]; dashed–[2, 0]; dotted–[2, 2]; dashed-dotted–[1, 1].

$$W(\epsilon) = \sum_i \frac{\Gamma(3 + l_x^i + l_y^i)}{\Gamma(\frac{3}{2} + l_x^i)\Gamma(\frac{3}{2} + l_y^i)} A_i^2 \epsilon^{l_x^i + (1/2)} (1 - \epsilon)^{l_y^i + (1/2)}. \quad (1)$$

Here, $\Gamma(z)$ is the Euler gamma function, l_x is the angular momentum between neutron-fragment (neutron-neutron) and l_y the angular momentum between the c.m. of the neutron-fragment pair (neutron-neutron pair) and the remaining neutron (fragment) for $W(\epsilon_{fn})$ [for $W(\epsilon_{nn})$], as illustrated in Fig. 2 of Ref. [13]. The decay amplitude for a certain configuration i is denoted A_i, with $\sum_i A_i^2 = 1$. In the analysis, the A_i^2 values were left as free parameters while $[l_x, l_y]$ where fixed to [0, 2], [2, 0], [1, 1], and [2, 2]. Note that the assumption of a closed $p_{3/2}$ subshell in the ^{10}Be core excludes the [1,1] component in the $W(\epsilon_{fn})$ analysis. The corresponding relative neutron-neutron partial waves may, however, have contributions from s, p, and d waves.

The fits of the experimental $W(\epsilon_{nn})$ and $W(\epsilon_{fn})$ spectra, using Eq. (1), are shown in Fig. 2. The resulting parameters are given in Table II.

For $0.5 \leq E_{fnn} \leq 1$ MeV, only the spectrum in Fig. 2(a) could be analyzed since the data for $W(\epsilon_{nn})$ are limited to the upper half of the spectrum. In this energy region, the distortions of the spectra from the experimental resolution are expected to be most important. Therefore, we performed a Monte Carlo simulation including the experimental resolution and using the theoretical shape of the $W(\epsilon_{fn})$ spectrum [solid line in Fig. 2(a)]. The histograms

TABLE II. Contributions, with statistical uncertainties, from different partial waves to $W(\epsilon_{fn})$ and $W(\epsilon_{nn})$ obtained in the vicinity of 2_1^+ and 2_2^+ states.

	l_x	l_y	A^2	χ^2/N
$W(\epsilon_{fn})$	0	2	0.30(5)	
0.5–1 MeV	2	0	0.29(5)	
2_1^+	2	2	0.41(7)	33.8/29
$W(\epsilon_{fn})$	0	2	0.45(3)	
2–3 MeV	2	0	0.46(3)	
2_2^+	2	2	0.09(4)	18.1/29
$W(\epsilon_{nn})$	0	2	0.44(7)	
2–3 MeV	2	0	0.24(3)	
2_2^+	2	2	0.00(4)	
	1	1	0.32(10)	23.9/23

in Fig. 2(a) show the result of such a simulation made under the assumption of an isotropic distribution of the emitted neutrons. The similarity between the full drawn curve and the simulation is evident and shows that the distortion due to the resolution is negligible compared to the statistical uncertainty and has, thus, limited influence on the derived parameters. The simulated data may also be used to predict the shape for $W(\epsilon_{nn})$, as shown in Fig. 2(b). Note the shift of the maximum in the $W(\epsilon_{nn})$ spectrum in Fig. 2(d) towards low ϵ_{nn}, which is a characteristic feature of a direct decay into $f + n + n$. It appears due to the strong nn interaction but disappears in a sequential decay via an intermediate resonance in the fn subsystem.

With a ^{12}Be ground-state wave function according to Refs. [10,12]

$$^{12}\mathrm{Be}(0^+) = {}^{10}\mathrm{Be} \otimes \left[\alpha(1s_{1/2})^2_{I=0} + \beta(0p_{1/2})^2_{I=0} + \gamma(0d_{5/2})^2_{I=0}\right], \quad (2)$$

and under the assumption that ^{10}Be may also be considered as a rigid core in the structure of the ^{14}Be(2^+) states, one arrives at the following representation:

$$^{14}\mathrm{Be}(2^+) = {}^{10}\mathrm{Be} \otimes \left[\begin{Bmatrix} \alpha_1(1s_{1/2})^2_{I=0} \\ \alpha_2(0p_{1/2})^2_{I=0} \\ \alpha_3(0d_{5/2})^2_{I=0} \end{Bmatrix} (0d_{5/2})^2_{I=2} + \begin{Bmatrix} \beta_1(0p_{1/2})^2_{I=0} \\ \beta_2(0d_{5/2})^2_{I=0} \end{Bmatrix} (1s_{1/2}, 0d_{5/2})_{I=2}\right]. \quad (3)$$

The relation between the internal structure of the resonance and the kinematical properties of decay products in the final state is complicated by the dynamical evolution of the system during the decay process. The 2^+ states in ^{14}Be, of the structure given in Eq. (3), decay to ^{12}Be + n + n with a strength proportional to the overlap integral of the corresponding wave functions, Eqs. (2) and (3), $(\alpha_1\alpha + \alpha_2\beta + \alpha_3\gamma$ for two neutrons with $l = 2$ and $\beta_1\beta + \beta_2\gamma$ for the

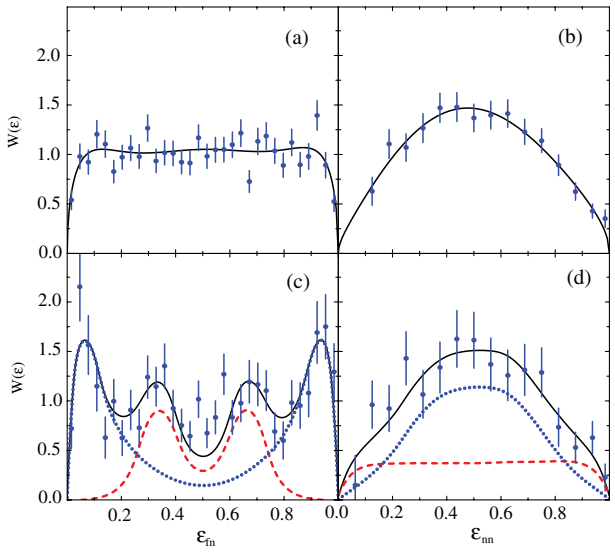

FIG. 3 (color online). Fractional energy spectra, $W(\epsilon_{fn})$ (a), (c) and $W(\epsilon_{nn})$ (b),(d), in ^{14}Be determined for $3 \leq E_{fnn} \leq 5$ MeV (a),(b) and $6 \leq E_{fnn} \leq 8$ MeV (c),(d). (a) and (b) The smooth solid lines are drawn as guides to the eyes. (c) and (d) The solid lines present a fit assuming sequential decay through $1/2^+$ and $5/2^+$ resonances in ^{13}Be. The experimental resolution was taken into account in the fits. The partial contributions are shown by dotted ($1/2^+$) and dashed ($5/2^+$) lines, respectively. See text for details.

$l = 0, 2$ pair), and the corresponding penetrability factors. The weights of different configurations of $^{12}\mathrm{Be} + n + n$ in the final states, given in Table II, suggest that the two valence neutrons building up the first 2^+ state mainly occupy the $0d_{5/2}$ shell, while they are in a mixed ($1s_{1/2}$, $0d_{5/2}$) configuration in the $E^* = 3.54(16)$ MeV state. The assignment of $I^\pi = 3^+$ to this state can be excluded due to the large [0, 2] and [2, 0] components found in the $W(\epsilon_{nn})$ distribution, which require that the total spin is zero for the two neutrons ($S = s_1 + s_2 = 0$).

The 2_1^+ state in ^{14}Be was first observed in a ^{14}C induced reaction [19] and later confirmed in three different experiments [15,16,20]. The observation of an excited state in ^{14}Be at $E^* = 4.1(2)$ MeV was announced in Ref. [20]. A plausible explanation for the difference in the resonance energies may be that the two overlapping states were not resolved in the experiment described in Ref. [20].

There are strong similarities between the excited states in the $N = 10$ isotones. The first excited state (2_1^+) of ^{14}Be at 1.54 MeV, found to be mainly a $(0d_{5/2})^2$ configuration [15,19], is similar to the 1.77 MeV state in ^{16}C and to the 1.98 MeV state in ^{18}O. The positions of the second 2^+ states are, in fact, also very close.

The $W(\epsilon_{fn})$ and $W(\epsilon_{nn})$ spectra obtained in the region around the $E^* = 5.25(19)$ MeV resonance are shown in Figs. 3(a) and 3(b). It is interesting to note that these correlation spectra show features that may be assigned both to democratic three-body breakup and sequential two-body decay via the $1/2 + (0.5$ MeV) and $5/2 + (2$ MeV) resonances in ^{13}Be [21]. The sharp increase at $\epsilon_{fn} \sim 0.1(0.9)$ may be ascribed to sequential emission via the $1/2^+$ state in ^{13}Be, while feeding to the 2 MeV resonance would contribute the center of the distribution. A consistent analysis, giving a spin-parity assignment including both types of decay mechanisms would, however, be ambiguous. Therefore, we only conclude that there is a resonance here and compare its position with states in other $N = 10$ isotones. One possibility would then be that it is an analog to the first 3^- state in $N = 10$ isotones with a $(0p_{1/2})^1(1s_{1/2}0d_{5/2})^3$ configuration, like the 3_1^- state in ^{18}O at $E^* = 5.10$ MeV, found to be strongly populated in proton inelastic scattering [22].

There is no sharp borderline between direct three-body and sequential two-body decays. However, for states at higher energies, one would expect that the decay via sequential neutron emission through intermediate states dominates. The correlation spectra shown in Figs. 3(c) and 3(d) from the region $6 < E_{fnn} < 8$ MeV show interesting patterns, in particular in the $W(\epsilon_{fn})$ spectrum, where the four maxima signal at least two intermediate states. To get a qualitative feeling for the expected spectral shape in the case of a sequential decay via ^{13}Be, a calculation within an R-matrix approach, with the approximation described in Ref. [23], was performed. This was done assuming a 1 MeV broad $^{14}\mathrm{Be}(3^-)$ resonance situated at 7 MeV, decaying into the known $1/2^+$ and $5/2^+$ resonances in ^{13}Be, with the experimental resolution taken into account. The maximum observed at low (high) ϵ value in the $W(\epsilon_{fn})$ spectrum was found to correspond perfectly to a sequential decay via the $1/2^+$ resonance. The second maximum appears, however, at an energy of the intermediate state about 15% higher than the known $5/2^+$ resonance to fit the data. The large E_{fnn} window, and possible decays to other intermediate states, might be a reason for this deviation. One should, e.g., note that there could be a decay branch to the narrow resonance at $E_r = 4.94(15)$ MeV in ^{13}Be, which has been observed in a multinucleon transfer reaction experiment [24], and most likely also this state may contribute. A more detailed description requires more detailed experimental information.

In conclusion, we have studied continuum states in ^{14}Be through inelastic scattering on protons. The analysis of the internal kinetic energy in the $^{12}\mathrm{Be} + n + n$ system, E_{fnn}, and energy correlations between decay products were performed. When the entire information is set into a global context, the presence of several resonances in the continuum is revealed. The earlier known 2_1^+ state is confirmed as a dominant $(0d_{5/2})^2$ configuration. The resonance at $E^* = 3.54$ MeV is identified as the 2_2^+ resonance. The structure of this state is shown to be predominantly ($1s_{1/2}$, $0d_{5/2}$). Analysis of the fragment-n-n correlations by the simple method proposed here can effectively be used for spin and parity assignments to the low-lying resonance states in

^{13}Li [25], ^{16}Be [26], and ^{26}O [27,28], recently observed and interpreted as showing dineutron decay.

The region around $E_{fnn} = 7$ MeV shows emission of neutrons with a pattern that might only be understood as a preferentially sequential decay via states in ^{13}Be.

The authors are indebted to S. Ershov for discussions. This work is partly supported by the Helmholtz International Center for FAIR within the framework of the LOEWE program launched by the State of Hesse, by the BMBF (Project No. 05P12RDFN8), through the GSI-TU Darmstadt cooperation contract, and by the Helmholtz Alliance EMMI. Financial support from the Swedish Research Council and the Spanish Ministry through the research Grant No. FPA2009-07387 is also acknowledged. B. J. is a Helmholtz International Fellow.

*Present address: National Superconducting Cyclotron Laboratory, MSU, East Lansing, MI, 48824, USA.

[1] Y. Blumenfeld, T. Nilsson, and P. Van Duppen, Phys. Scr. T **T152**, 014023 (2013).
[2] T. Suzuki *et al.*, Nucl. Phys. **A658**, 313 (1999).
[3] S. Ilieva *et al.*, Nucl. Phys. **A875**, 8 (2012).
[4] M. Zahar *et al.*, Phys. Rev. C **48**, R1484 (1993).
[5] M. Labiche *et al.*, Phys. Rev. Lett. **86**, 600 (2001).
[6] S. Takeuchi *et al.*, Phys. Lett. B **515**, 255 (2001).
[7] P. Descouvemont, Phys. Rev. C **52**, 704 (1995).
[8] I. J. Thompson and M. V. Zhukov, Phys. Rev. C **53**, 708 (1996).
[9] C. Forssén, V. D. Efros, and M. V. Zhukov, Nucl. Phys. **A706**, 48 (2002).
[10] F. C. Barker, J. Phys. G **2**, L45 (1976).
[11] S. Shimoura *et al.*, Phys. Lett. B **560**, 31 (2003).
[12] H. T. Fortune and R. Sherr, Phys. Rev. C **85**, 051303(R) (2012).
[13] H. T. Johansson *et al.*, Nucl. Phys. **A847**, 66 (2010).
[14] Th. Blaich *et al.*, Nucl. Instrum. Methods Phys. Res., Sect. A **314**, 136 (1992).
[15] T. Sugimoto *et al.*, Phys. Lett. B **654**, 160 (2007).
[16] Y. Kondo, PhD Thesis, Tokyo Institute of Technology, 2007.
[17] R. I. Jibuti, N. B. Krupennikova, and V. Yu. Tomchinsky, Nucl. Phys. **A276**, 421 (1977).
[18] L. M. Delves, Nucl. Phys. **20**, 275 (1960).
[19] H. G. Bohlen *et al.*, Nucl. Phys. **A583**, 775 (1995).
[20] A. A. Korsheninnikov *et al.*, Nucl. Phys. **A616**, 189 (1997).
[21] Yu. Aksyutina *et al.*, Phys. Rev. C **87**, 064316 (2013).
[22] J. Escudié, R. Lombard, M. Pignanelli, F. Resmini, and A. Tarrats, Phys. Rev. C **10**, 1645 (1974).
[23] F. C. Barker, Phys. Rev. C **59**, 535 (1999).
[24] A. V. Belozyorov *et al.*, Nucl. Phys. **A636**, 419 (1998).
[25] Z. Kohley *et al.*, Phys. Rev. C **87**, 011304 (2013).
[26] A. Spyrou *et al.*, Phys. Rev. Lett. **108**, 102501 (2012).
[27] Z. Kohley *et al.*, Phys. Rev. Lett. **110**, 152501 (2013).
[28] C. Caesar *et al.*, Phys. Rev. C **88**, 034313 (2013).